

Observation and Simulation of fine particulate matter pollution during G20 in Hangzhou

Wei Dai¹, Huan Yu¹

¹ School of Environmental Science and Engineering, Nanjing University of Information Science and Technology, Nanjing, 210044, China

ABSTRACT: We research the size distribution by SMPS at the National Reference Climatological Station and simulation $PM_{0.1}$ number concentration from August 14 to 21, September 2 to 7, September 16 to 23 by WRF-Chem. $PM_{0.01}$, $PM_{0.1}$, PM_1 decreased a lot compared to those before and after the control period. Four typical NPF events occurred out of 7 days in Phase 1 and Phase 2, probably due to low condensation/coagulation sink. The $PM_{0.01}$ peak concentration around 11:00 AM was enhanced on the NPF days by a factor of 4 compared to the non-NPF days. The cause of pollution is similar, meteorology conditions were disadvantage to diffusion. During the three pollution incidents the contribution proportion of local $PM_{0.1}$ increase from 62.87%-75.22% to 83.52%-87.38%.

*Emission control strategy:

- 1) power plant emission reduction from August 24 to September 6
- 2) "odd-even" on-road vehicle restriction (i.e. 50% vehicle emission reduction) from August 28 to September 6
- 3) industrial VOC reduction from industrial sectors (e.g. refinery and chemical processes/facilities) from August 31 to September 6

***WRF-CHEM model setup:** The WRF-Chem model (version 3.6.1) in this study used two nested domains. Domain 1 and 2 covered eastern China and the region under emission control in the 2016 G20 summit, respectively. The grid points for Domain 1 are 85×95 with a horizontal resolution of 12km. The grid points for domain 2 are 118×142 with a horizontal resolution of 4 km. Gas phase and aerosol schemes in our simulation are CBM-Z and MOSAIC, respectively.

RESULTS AND DISCUSSION

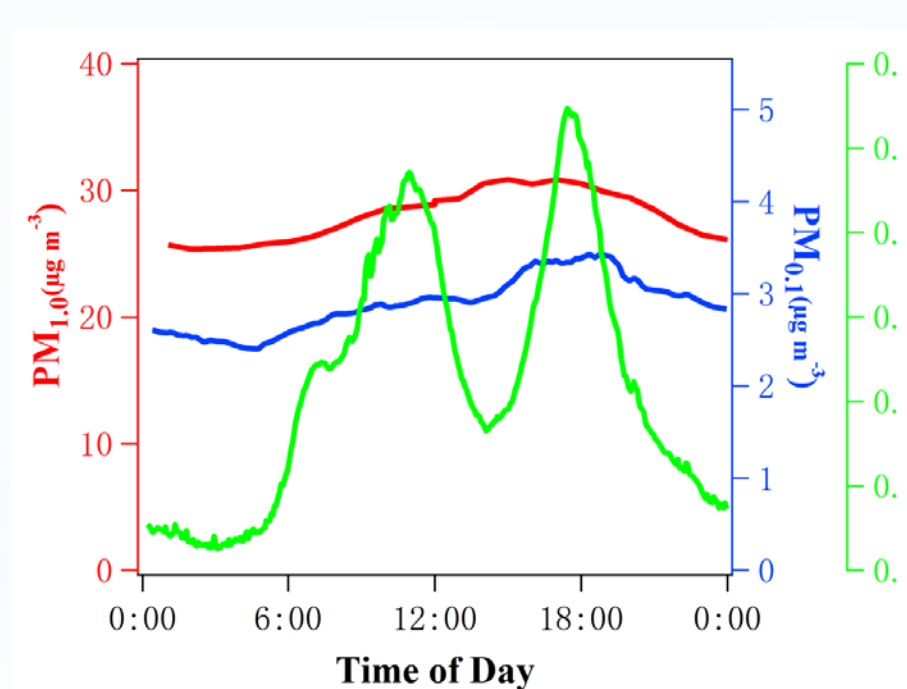


Fig. 1. Mean diurnal variation of PM_1 (red line), $PM_{0.1}$ (blue line) and $PM_{0.01}$ (green line) during the observation period.

Figure 1 shows that during the observation period, the mass concentration of $PM_{0.1}$ was $2.9 \pm 0.3 \mu\text{g}/\text{m}^3$ that accounted for $10.3 \pm 0.5\%$ in PM_1 . PM_1 and $PM_{0.1}$ showed a similar unimodal diurnal variation. Different from PM_1 and $PM_{0.1}$, $PM_{0.01}$ showed a trimodal diurnal variation (Figure 1). Peak concentrations were 0.25 , 0.47 and $0.55 \text{ ng}/\text{m}^3$, respectively, in compared with $0.13 \pm 0.04 \text{ ng}/\text{m}^3$ during the nighttime.

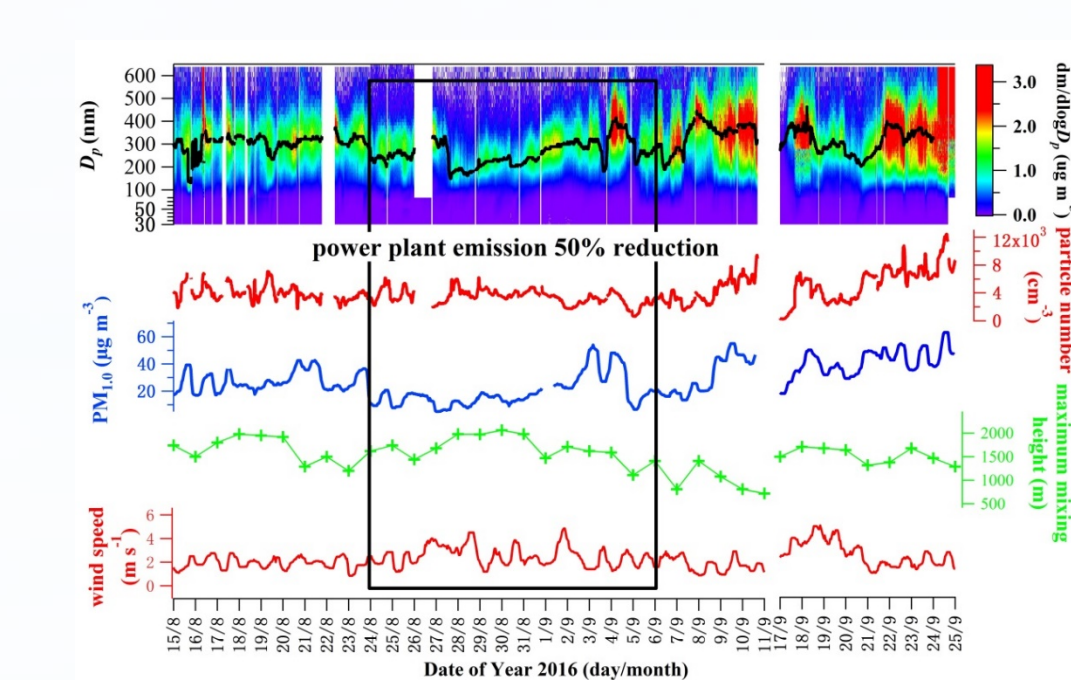


Fig. 2. from upper to lower: mass spectra, median diameter (black line), 100-1000 nm particle number concentration (red line), PM_1 mass concentration (blue line) of atmospheric aerosols, ground level wind speed and daily maximum boundary layer height (BLH) during the observation period. The black box highlights the power plant emission control period during G20.

PM_1 mass concentration was found to be decreased during the coal-fired power plant emission control period from August 31 to September 6. Excluding the two pollution episodes on September 3 and September 4, which was 40% and 58% lower than the mean concentrations before and after the control period, respectively. Due to bad meteorology diffusion conditions that the decrease of PM_1 was mainly benefited from the coal-fired power plants emission reduction. The number concentration of 100-1000 nm particles was $4000 \pm 800 \text{ cm}^{-3}$ during our observation period and did not exhibit statistically lower concentrations during the control period. The median sizes of PM_1 decreased significantly to $253 \pm 40 \text{ nm}$ during the control period, which was 52 nm and 80 nm lower than those before and after the control period, respectively. During the power plant emission control period the growth of ambient particles was slower with less secondary contribution from gas phase.

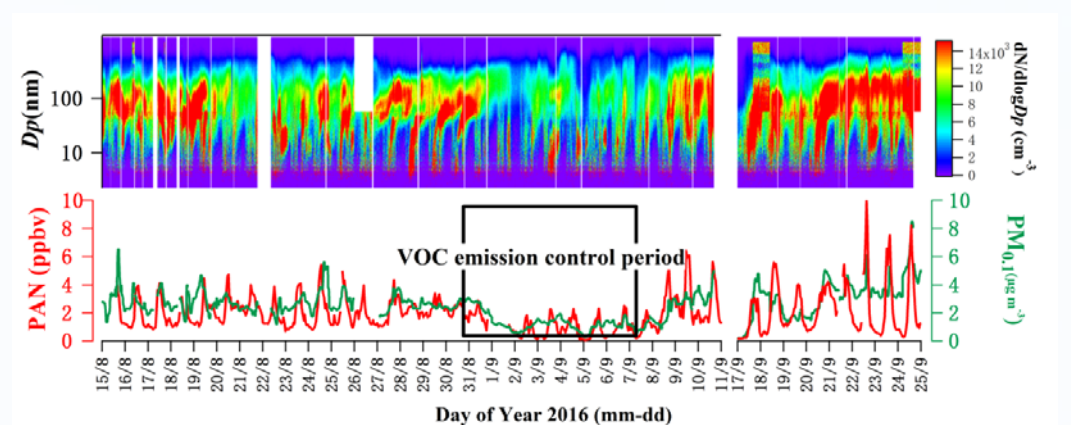


Fig. 3. Upper: particle number size spectra during the observation period. Lower: mass concentration of $PM_{0.1}$ (green line) and PAN (red line) during the observation period. The black box highlights the VOC emission control period.

After the enforcement of VOC emission control (August 31st – September 6th), $PM_{0.1}$ mass concentration decreased significantly by 53% to $1.3 \pm 0.6 \mu\text{g}/\text{m}^3$. PAN showed similar decrease during the same period. Furthermore, the correlation coefficient between PAN and $PM_{0.1}$ was 0.85. Therefore, the correlation suggested that $PM_{0.1}$ and PAN were produced from the same atmospheric oxidation process of VOC emission.

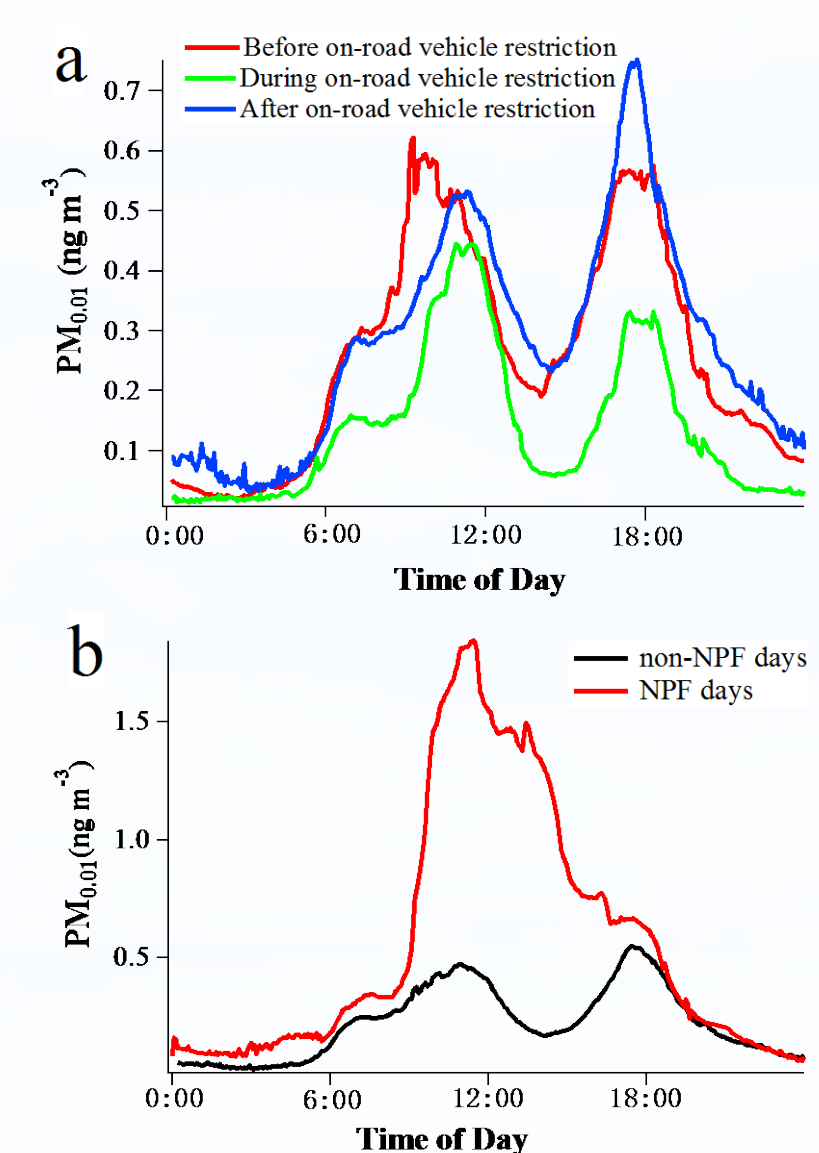


Fig. 4. Mean diurnal variations of $PM_{0.01}$ (a) before (red line), during (green line) and after (blue line) the "odd-even" on-road vehicle restriction and (b) on NPF days (red line) and non-NPF days (black line).

Previous source apportionment studies have found that vehicle emission is the most important contributor to PM_1 in Hangzhou. However, we did not observe visible PM_1 reduction before and after on-road vehicle restriction. Instead, we observed that sub-10 nm nanoparticle concentrations in rush hours around 07:00 and 18:00 decreased dramatically by 48% and 42% after the enforcement of "odd-even" on-road vehicle restriction (Figure 4a). The second $PM_{0.01}$ peak around 11:00 AM, however, decreased by only 16% with the vehicle restriction. $PM_{0.01}$ diurnal variations in Figure 4b showed that NPF events enhanced the second $PM_{0.01}$ peak on the NPF days by a factor of 4 compared to the non-NPF days. The evidences above indicated that the vehicle emission and the regional NPF events were the two sources of nanoparticles below 10nm in the urban atmosphere of Hangzhou. The emission control did not suppress NPF occurrence completely. On the 7 days before the enforcement of VOC emission reduction (i.e. Phase 1 and Phase 2), there were 4 typical NPF events on August 25, 27, 28 and 29. It is possible that PM_1 and thus condensation/coagulation sink for nucleation precursors and clusters were reduced in the Phase 1 and 2 period. On the other hand, the supply of VOCs, as nucleation precursors, was still high in these two phases.

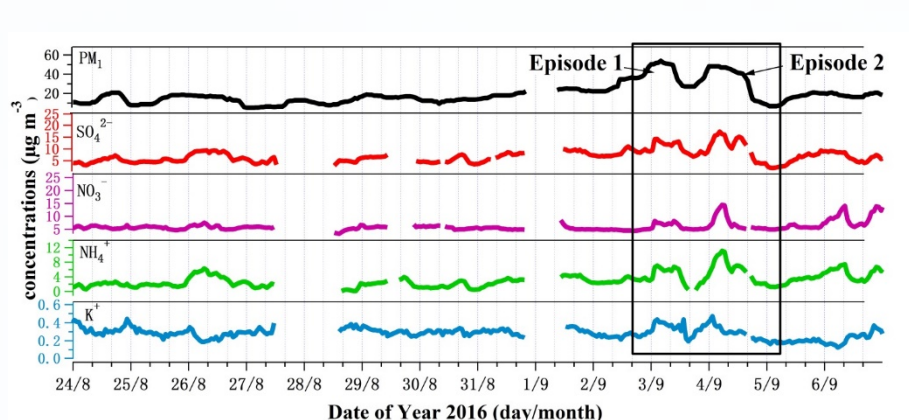


Fig. 5. Mass concentrations of PM_1 (black line) and water-soluble inorganic ions (SO_4^{2-} , red line; NO_3^- , purple line; NH_4^+ , green line; K^+ , blue line) during the emission control period. The black box shows the two PM episodes on September 3, 2016 (episode 1) and September 4, 2016 (episode 2).

Although the most strict emission control scheme was enforced during the Phase 3 period from August 31st to September 6, two PM_1 episodes were still observed on September 3 and September 4 (Figure 2). When PM_1 reached its maximum in episode 1, the sum of secondary inorganic ions (SO_4^{2-} , NO_3^- and NH_4^+) increased by ~100% compared to the rest of phase 3 days. The boost of secondary inorganic ions accounted for 47% of the total increment in PM_1 . In episode 2, the sum of SO_4^{2-} , NO_3^- and NH_4^+ increased by 152% and accounted for 62.5% of the total increment of PM_1 . The concentration of K^+ increased by 21% and 23% in episodes 1 and 2, respectively. It indicated that secondary inorganics and biomass burning are important contributors in the two episodes.

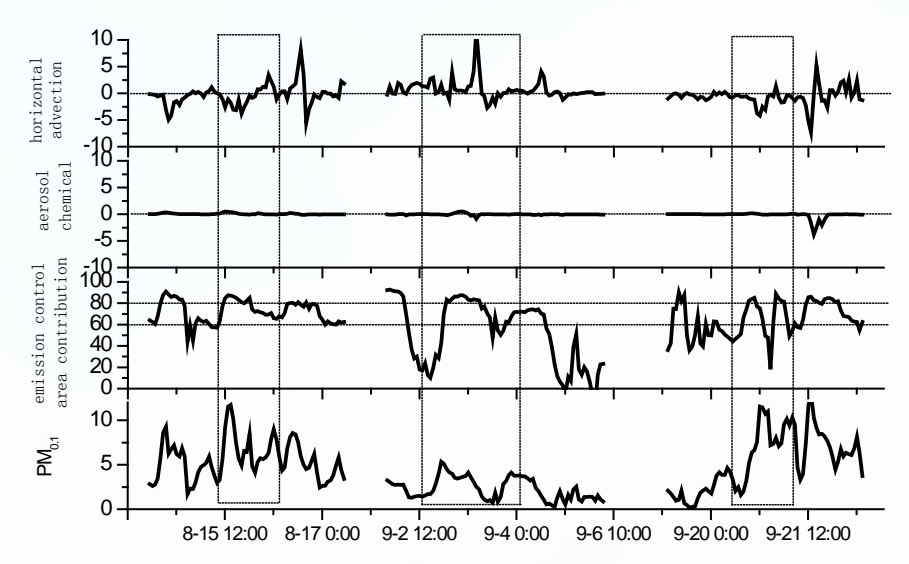


Fig. 6 from upper to lower: horizontal advection ($\mu\text{g}/\text{m}^3 \cdot \text{h}$), aerosol chemical ($\mu\text{g}/\text{m}^3 \cdot \text{h}$), emission control area contribution (%), PM_1 number concentration ($10^3/\text{cm}^3$) during the emission control period. The black box highlights three $PM_{0.1}$ pollution incidents

We compare the three $PM_{0.1}$ pollution processes before, during, after the G20 emission control strategy, the cause of pollution is similar. $PM_{0.1}$ pollutant can transport between the grid, when we restricted area at G20 emission control strategy area, find out that $PM_{0.1}$ pollutant transport from surrounding area. During the three pollution incidents the contribution proportion of local $PM_{0.1}$ increase from 62.87%-75.22% to 83.52%-87.38%, but the number concentration of $PM_{0.1}$ from outer emission control strategy area unchanged. So, $PM_{0.1}$ pollutant transport from emission control strategy were led to summer pollution incident in Hangzhou. Furthermore, the pollution process during the emission control period is more dependent on meteorology conditions.

Table 1 comparison of control and uncontrol area contribution of $PM_{0.1}$ number concentration ($10^3/\text{cm}^3$) at Hang Zhou station

	concentration ($10^3/\text{cm}^3$) at Hang Zhou station		
	Hang Zhou station	Control area	Uncontrol area
before	mean 5.61	4.23 (75.22%)	1.38 (24.78%)
	peak 11.59	10.13 (87.38%)	1.46 (12.62%)
	difference	5.9	0.08
during	mean 1.67	1.05 (62.87%)	0.62 (37.13%)
	peak 3.18	2.66 (83.52%)	0.52 (16.48%)
	difference	1.61	-0.1
after	mean 5.47	3.75 (68.56%)	1.72 (31.44%)
	peak 11.58	9.87 (85.27%)	1.71 (14.73%)
	difference	6.12	-0.01

We compare the three $PM_{0.1}$ pollution processes before, during, after the G20 emission control strategy, the cause of pollution is similar. $PM_{0.1}$ pollutant can transport between the grid, when we restricted area at G20 emission control strategy area, find out that $PM_{0.1}$ pollutant transport from surrounding area. During the three pollution incidents the contribution proportion of local $PM_{0.1}$ increase from 62.87%-75.22% to 83.52%-87.38%, but the number concentration of $PM_{0.1}$ from outer emission control strategy area unchanged. So, $PM_{0.1}$ pollutant transport from emission control strategy were led to summer pollution incident in Hangzhou. Furthermore, the pollution process during the emission control period is more dependent on meteorology conditions.

CONCLUSION

We research the size distribution by SMPS at the National Reference Climatological Station and simulation $PM_{0.1}$ number concentration from August 14 to 21, September 2 to 7, September 16 to 23 by WRF-Chem. We compare the cause and the source of fine particulate matters by before, during, and after the 2016 G20 emission control strategy get these conclusions:

- (1) Power plant emission reduction of 50% had suppressed the growth of particles and decreased PM_1 by 40% and 58% compared to those before and after the control period. Sub-10 nm nanoparticle concentrations declined by 48% and 42% in morning and evening rush hours, respectively, after the implementation of 50% on-road vehicle reduction. 100% VOC emission reduction from industrial sectors enforced resulted in a 53% reduction of $PM_{0.1}$ concentration.
- (2) Four typical NPF events occurred out of 7 days in Phase 1 and Phase 2, probably due to low condensation/coagulation sink. This is different from the NPF events after the emission control period when both nucleation precursor and coagulation sink were high.
- (3) The NPF event was found to be an important source of nanoparticles below 10nm. The $PM_{0.01}$ peak concentration around 11:00 AM was enhanced on the NPF days by a factor of 4 compared to the non-NPF days.
- (4) We compare the three $PM_{0.1}$ pollution processes before, during and after the G20 emission control strategy, the cause of pollution is similar, controlled by anticyclone in 850hPa, the surface wind speed was weak, these conditions were disadvantage to pollutants diffusion. The $PM_{0.1}$ pollutant come from G20 emission control strategy area. During the three pollution incidents the contribution proportion of local $PM_{0.1}$ increase from 62.87%-75.22% to 83.52%-87.38%, but the number concentration of $PM_{0.1}$ from outer emission control strategy area unchanged.